PERGAMON

Carbon 38 (2000) 183–197

CARBON

Recent development of carbon materials for Li ion batteries

M. Endo*, C. Kim, K. Nishimura, T. Fujino, K. Miyashita

Faculty of Engineering, Shinshu University, 500 Wakasato, Nagano 380-8553, Japan

Received 19 April 1999; accepted 24 June 1999

Abstract

Lithium ion secondary batteries are currently the best portable energy storage device for the consumer electronics market. The recent development of the lithium ion secondary batteries has been achieved by the use of selected carbon and graphite materials as an anode. The performance of lithium ion secondary batteries, such as the charge/discharge capacity, voltage profile and cyclic stability, depend strongly on the microstructure of the anode materials made of carbon and graphite. Due to the contribution of the carbon materials used in the anode in last five years, the capacity of the typical Li ion battery has been improved 1.7 times. However, there are still active investigations to identify the key parameters of carbons that provide the improved anode properties, as carbon and graphite materials have large varieties in the microstructure, texture, crystallinity and morphology, depending on their preparation processes and precursor materials, as well as various forms such as powder, fibers and spherule. In the present article, we describe the correlation between the microstructural parameters and electrochemical properties of conventional and novel types of carbon materials for Li ion batteries, namely, graphitizable carbons such as milled mesophase pitch-based carbon fibers, polyparaphenylene-based carbon heat-treated at low temperatures and boron-doped graphitized materials, by connecting with the market demand and the trends in Li ion secondary batteries. The basic scientific theory can contribute to further developments of the Li ion batteries such as polymer batteries for consumer electronics, multimedia technology and future hybrid and electric vehicles.

Keywords: A. Intercalation compounds; D. Electrochemical properties

1. Introduction

Among the metals, lithium has great promise as an electrode material of batteries that can combine the lightest weight with high voltage and high energy density. Because lithium possesses the lowest electronegativity of the standard cell potential −3.045 V in the existing metals, it is the anode material that donates electrons the most easily to form positive ions [1]. However, the negative electrode of lithium metal has serious problems as secondary battery use, since it does not have a long enough cyclic life and there are safety aspects that need to be considered due to the dendrite formation on the surface of lithium metal electrode during charge/discharge cycles. In order to solve these problems a ''locking-chair'' concept has been established, in which the intercalation phenomena has been used as an anode reaction for lithium ion secondary batteries [2–5]. The intercalation compound of lithium metal into graphite by vapor transport was first synthesized by Herold [6] as a graphite intercalation compound (GIC) with stage structure. Since then, extensive study has been performed to investigate the staging structure and charge transfer phenomena of the Li-GIC compounds, which have the composition of Li_xC_6, where $0 \leqslant x \leqslant 1$, and $x=3$ under high pressure, into order and disordered host materials [7–12].

In the rechargeable lithium ion batteries based on the ''rocking chair'' or ''shuttle cock'' concepts, the lithium ions intercalates have to shift back and forth easily between the intercalation hosts of the cathode and anode. Thus, the lithium ion secondary battery mainly consists of a carbonaceous anode and a lithium transition metal oxide such as $LiCoO_2$, $LiNiO_2$ and $LiMn_2O_4$ as the cathode, as demonstrated in Fig. 1a. The anode on Cu foil and the cathode on Al foil are formed into spiral or plate folded shapes that give the US18650 cylindrical type (18 mm ϕ and 650 mm high, Fig. 1b) and rectangular cells, respectively. Between these two electrodes is placed a porous polymer separator of polyolefin of about 25 μm thickness,

*Corresponding author. Tel.: +81-26-2269-5201; fax: +81-26-223-7754.

E-mail address: endo@endomoribu.shinshu-u.ac.jp (M. Endo)

0008-6223/00/$ – see front matter
PII: S0008-6223(99)00141-4

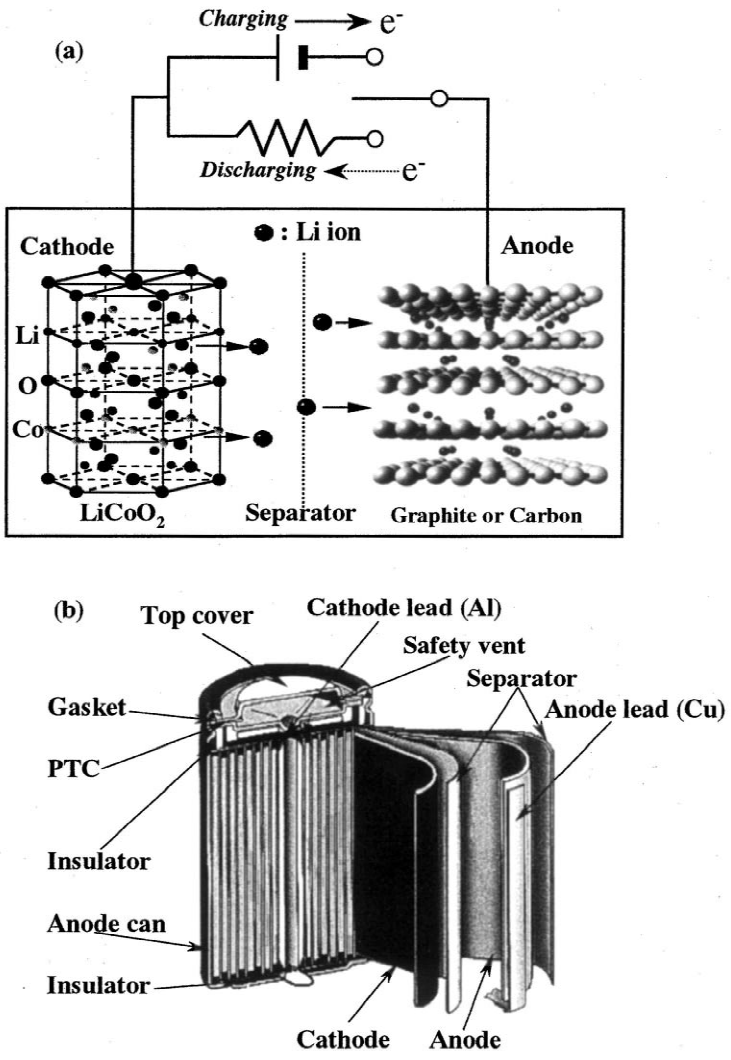

Fig. 1. (a) Charging-discharging mechanism of Li ion secondary battery and (b) the structures of practical cell (b) [13,14].

made by polyethylene (PE) and polypropylene (PP) (Fig. 1b) [13,14]. Fig. 2 shows the SEM photograph of the anode, in which carbon sheets are formed on both side of the Cu foil lead. The electrolyte is an organic liquid such as PC, EC+DEC or a recently developed gel-type polymer, which is stable under high voltages. In the electrolyte lithium salt such as $LiClO_4$, $LiBF_4$ and $LiPF_6$ is dissolved.

The theoretical lithium storage capacity of a graphite anode for a Li ion secondary battery has been considered to be 372 mAh/g, corresponding to the first stage LiC_6-GIC. The charge/discharge total reactions and the anode reaction based on Li^+ intercalation and deintercalation are shown as follows [15]:

$$LiCoO_2 + yC \underset{\text{Discharge}}{\overset{\text{Charge}}{\rightleftarrows}} Li_{1-x}CoO_2 + Li_xCy \quad (1)$$

$$yC + xLi + xe^- \underset{\text{Discharge}}{\overset{\text{Charge}}{\rightleftarrows}} Li_xC_y \quad (2)$$

On the other hand, disordered carbons with Li storage capacity exceeding the theoretical capacity have been reported. This phenomenon is still difficult to explain by the above-mentioned GIC science, and new schemes needed to be established.

Various types of carbonaceous materials have been investigated experimentally and theoretically as the potential anode materials ranging from highly ordered graphites to disordered carbons. Investigations have focused on improving the specific capacity, cyclic efficiency and the cyclic lifetime of the energy storage devices. For the anode material of the lithium ion batteries the microstructure and morphologies must be controlled for practical

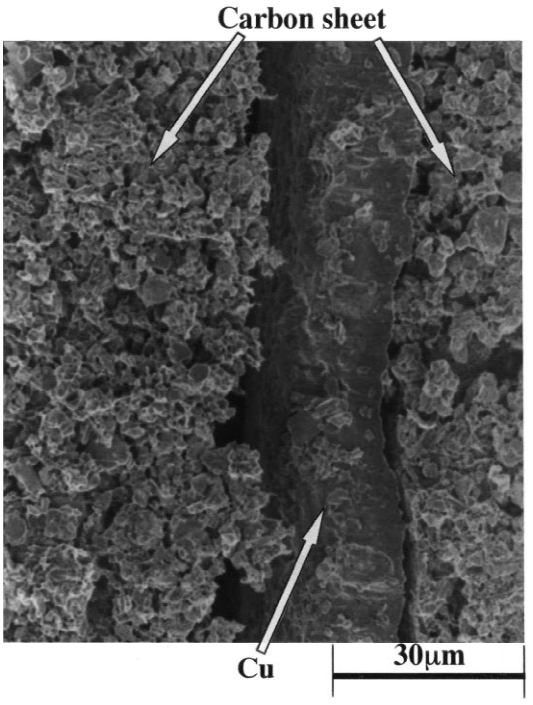

Fig. 2. SEM photograph of the carbon anode sheets formed on both the sides of a Cu foil lead.

devices. It has been well known that the performances of lithium ion batteries depend strongly on the thermal history and morphology of carbon and graphite materials used for the anode [16]. Much more effort has been paid to the identification the key parameters of the carbon and graphite materials used for the battery. Because carbon and graphite materials have large variety in their microstructure, texture, crystallinity and morphology, it has been important to design and choose the anode material from a wide variety in order to get better battery performances [17–19]. Two typical types of carbon materials, highly-ordered graphite heat-treated at high temperatures such as 3000°C and non-graphitizable carbon heat-treated at low temperatures such as 1100°C, have been used in the anode in commercial batteries. The precursor materials include cokes, polymers, fibers and many others. Also, the insertion behavior and the mechanism of the lithium ions into various kinds of carbon and graphite hosts have been extensively studied both experimentally and theoretically [20–25]. In particular, the lithium insertion mechanism and electrochemical properties in low temperature carbons, unlike the case of well-ordered graphite, are not yet fully understood as described before, and the perfect analysis is indispensable for practical use. The low temperature forms of carbon might be very promising for the following stage of Li ion battery because of their superior capacity. Also, the low temperature forms of carbon would be preferable in order to decrease the amount of electrical energy used in anode production, since graphite materials for anode application are heat-treated at around 3000°C and about 200 ton/month are consumed.

In the present review, we discuss the recent achievements of carbon anode materials and their structural design for better performances of lithium ion batteries. In the past 6 years, since commercialization started, the discharge capacity of Li ion batteries has been improved 1.7 times, from 900 to 1500 mAh for a typical US 18650 type cell, and is expected to be as high as 1900 mAh/cell soon. This large improvement in capacity has been recognized mainly due to the contribution of carbon technology to the negative electrode. Further scientific, as well as technical, accumulation can develop an advanced Li ion battery, such as the polymer type thin card battery soon to be on the market, and also the technology can be used for future full electric vehicle (EV) applications.

2. Present status and future trends in Li ion battery market

Li ion secondary batteries are currently the best energy storage devices for portable consumer electronics, in comparison with other conventional batteries, because of the high energy density as shown in Fig. 3. They were first developed and commercialized by Sony in 1990 and have been used in a wide range of portable stationary such as notebook computers, cellular phones and digital video cameras, etc. [26]. As seen in Fig. 3, basically, lithium ion secondary batteries have the advantage of having 1.5 times the volume, 1.5~2 times the weight of energy density, and approximately 3 times the voltage (~3.6 V) than NiCd batteries (1.2 V) [26]. The high performances of the

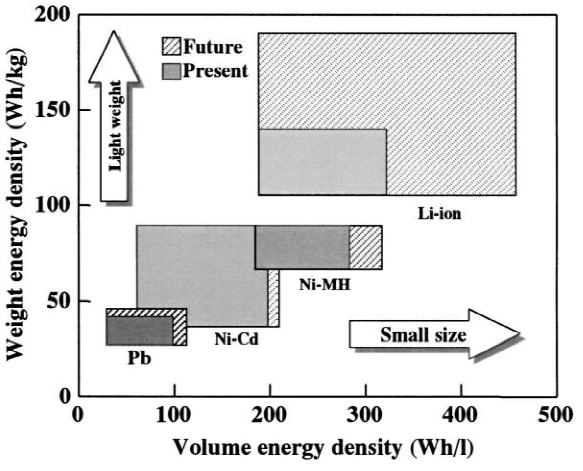

Fig. 3. Energy density of various kinds of secondary batteries, present ( ) and future ( ) based on electrodes.

battery have been supporting the recent large developments in cellular phones, personal computers with color liquid crystal device (LCD) and high speed CPU as shown in Fig. 4a and b [27,28]. For example, 95 g weight of cellular phones with 46 mm width, 22 mm length and 11 mm thickness rectangular Li cell can operate during 6 h for talk and 600 h for stand-by.

Fig. 5 is the recent transition in production amount of small size secondary batteries in Japanese market. Especially, the Li ion battery produced in Japan have about 99% of the world market, and the yearly production has reached 2.0 billion dollar in 1997 which is about twice those for NiMH and NiCd's. Because of the strong demand from consumer electronics market and also electric vehicle, Li ion battery technologies have been required to achieve further development in energy density, output current, safety and cost. It has been expected from the PC market that the 10 h of operation and 1000 cycle life corresponding to the apparatus life. The battery enable to be settled in PC (personal computer) and cellular phone will make us forget the battery charging. Li ion polymer type battery, described later and which will become the main type in these market fields, has the possibility to challenging for such a request as well as for future full EV application.

3. Voltage profiles of carbon electrodes

In the electrochemical cell used in the present article, the electrodes of carbon materials are positive electrodes since the counter electrode is lithium metal, therefore lithium intercalation to carbon corresponds to the discharge process, whereas the deintercalation of lithium ions is a charge process.

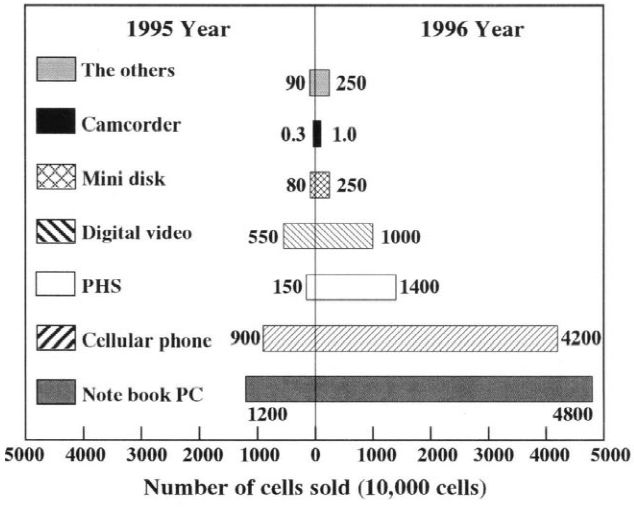

(a)

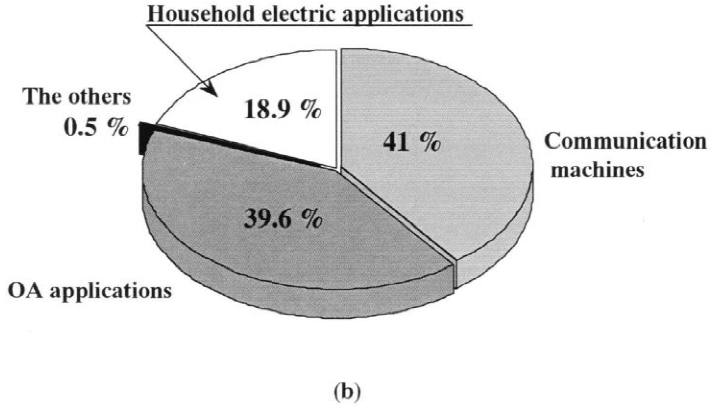

(b)

Fig. 4. (a) Number of cells sold in the world market in 1995 and 1996, and (b) the use of Li ion battery (data from Battery Association of Japan (1997)).

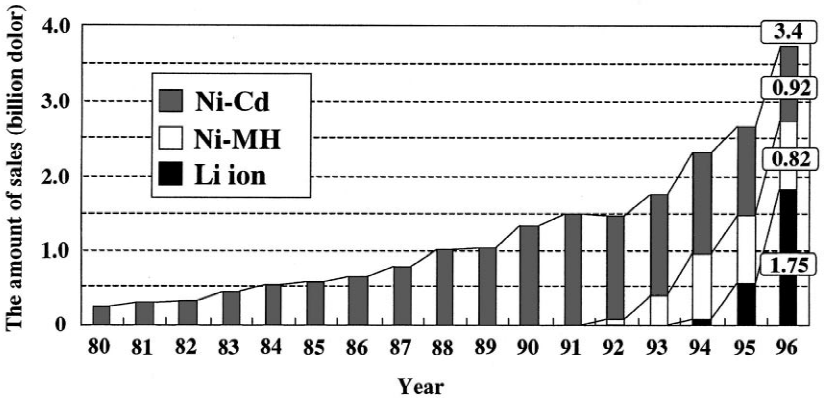

Fig. 5. The transition of production amount (in dollars) of the various types of secondary batteries (data from International Trade and Industry Statistics of MITI, 1997).

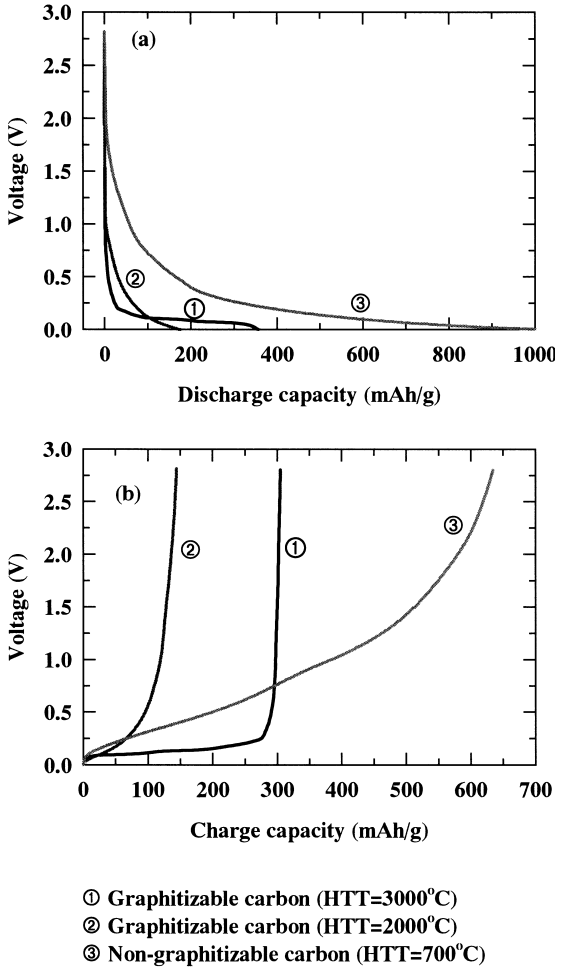

Fig. 6. Plots of voltage vs. reversible capacity for (a) the second discharge and (b) charge cycle of representative carbon and graphite samples, ① graphitizable carbon heat-treated at 3000°C, ② graphitizable carbon heat-treated at 2000°C, ③ non-graphitizable carbon heated at 700°C.

Fig. 6 shows the voltage profiles for lithium/carbon electrochemical cells made from representative carbon and graphite materials [21]. The graphite electrode cell gives a reversible capacity of 280~330 mAh/g, and lithium discharge/charge plateau at below 0.2 V was reproduced [9,23]. In the first cycle, all types of carbon materials show the irreversible capacity at about 0.8 V due to electrolyte decomposition and formation of solid electrolyte interphase [29]. Then, after 2nd cycles the irreversible capacity is much reduced, and the electrode exhibits stable cyclic properties. Among many types of carbon electrodes, well-ordered graphites are currently becoming one of the representatives for the industrial standard because of its long plateau in voltage profile and for low electrode potential relative to lithium metal. However, a major disadvantage of the graphite system has the limited lithium storage capacity as about 310 mAh/g in current commercial cell, which is much less than 372 mAh/g corresponding to LiC_6. On the other hand, soft carbons heat-treated at temperature (500~1000°C) give a reversible capacity of near 700 mAh/g, and indicate characteristic plateau in discharge/charge properties at about 1.0 V, as well as hysteresis in voltage profile about 0.0 V [21,22,30]. Furthermore, hard carbons heat-treated at temperatures around 1100°C give a reversible capacity of 600 mAh/g, but have the small irreversible capacity and hysteresis

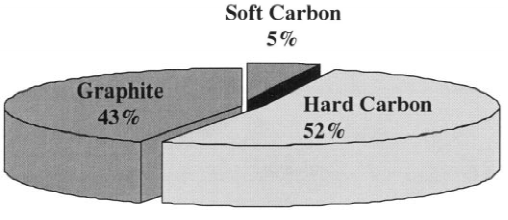

Fig. 7. Carbon materials used for commercial Li ion secondary batteries used in the market in 1996.

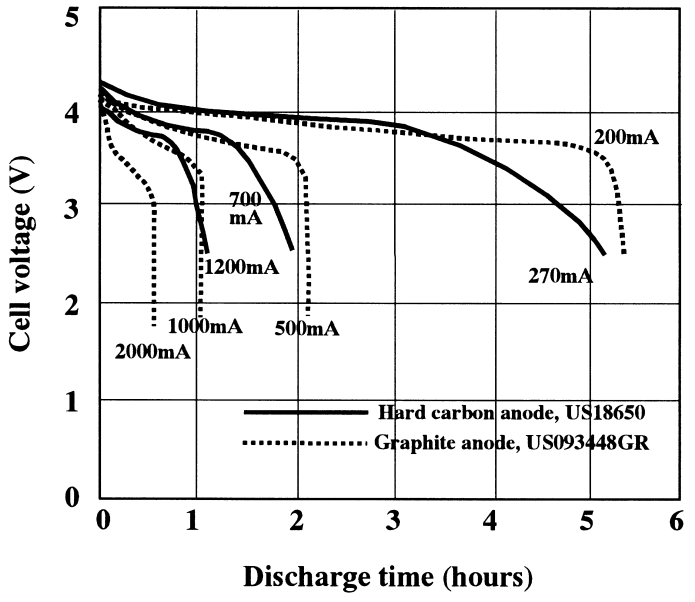

Fig. 8. Discharge characteristics of typical two types of commercial cell [13].

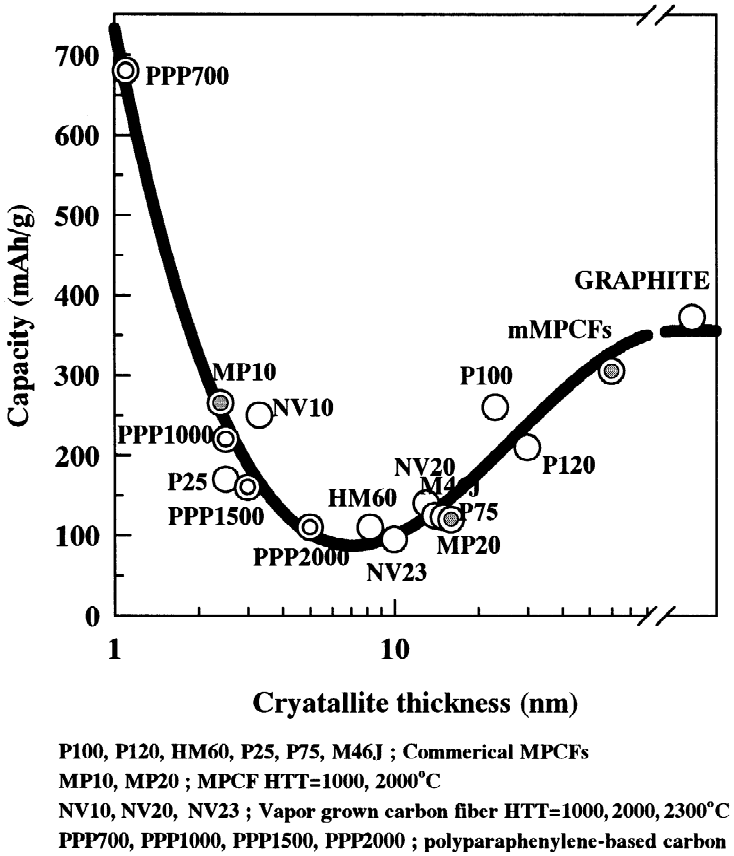

Fig. 9. Charge capacity of the various kinds of carbon fiber and PPP-based carbon electrodes at the second cycle as a function of crystallite thickness, $Lc_{(002)}$, determined by X-ray diffraction analysis [16]. Dahn et al. [21] also proposed three regions of lithium ion insertion capacity by the heat treatment temperatures of carbon materials.

between charge and discharge in the voltage profile [21,30,31].

In the commercial cell well-ordered graphites such as mesocarbon microbeads (MCMB) hat-treated at 3000°C and natural graphite, and non-graphitizing carbons (hard carbon) heat-treated presumably at around 1100°C have been mainly used as indicated in Fig. 7. These graphite and hard carbon have the capacity, in charge, of 310 mAh/g and 400 mAh/g, respectively [32]. As shown in Fig. 8, these different anodes show different out-put properties with constant and slightly inclined potential for discharging in the commercial cell, which has been recognized to be more suitable for cellular phones and EV battery applications, respectively.

4. Effect of microstructure of carbon anode on the capacity

Fig. 9 shows the second cycle charge capacity as a function of crystal thickness, Lc_{002}, on various carbon fiber and PPP (polyparaphenylene)-based carbon electrodes [16]. Well-ordered graphites ($Lc_{002}>20$ nm) and low crystalline materials ($Lc_{002}<3$ nm) have a larger capacity. However, intermediate crystallite sizes (~10 nm) possess minimum capacity. Dahn et al. [21] reported the same kind of dependency on charge capacity as a function of heat treatment temperatures. Of particular interest in these capacity dependencies, is the highly disordered PPP-700 carbon (heat-treated at 700°C) exhibits a large charge capacity of 680 mAh/g or more [20]. Namely, as Lc_{002} becomes smaller from graphite crystal, the charge capacity decreases monotonically up to the Lc_{002} values of about 10 nm, which is based on the Li^+ intercalation to graphite and turbostratic carbon structures. On the other hand, for $Lc_{002}<10$ nm, a different process of doping and undoping of Li ion may occurs, and this process is largely enhanced by decreasing the crystallite thickness. For Lc_{002} around 10 nm, both reaction processes occur incompletely, which might cause a minimum in the capacity.

The extremely enhanced charge capacity in PPP-700 can be explained as follows, based on in situ Raman spectroscopy (Fig. 10a and b) [33] and NMR experiments [20]. The results of lineshape analysis for the high frequency mode near 1600 cm^{-1} are expressed in Fig. 11, which provides interesting information about the Raman frequency shift in the Li/PC/PPP-700 battery system during discharging and charging. The high frequency peak position as a function of electrode voltage, in the range between approximately 2.8 and 0.0 V for both of the discharging and charging processes, is reflected in the Li^+ uptake and release in PPP-700. It is worthwhile to note that the curves have thresholds at about 1.0 V, and are divided into two zones by the threshold voltages. That is to say, in Zone I (2.8~1.0 V) the Raman peak wave number shows no change with decreasing voltage up to 1.0 V, and the other Zone II (1.0~0.3 V) corresponds to the downshift of the wave number with decreasing the voltage for discharging. On the other hand, for charging, the change in peak position takes place almost reversibly with some hysteresis effect indicating some amount of residual Li. The present results suggest that in Zones I and II the Li^+ ions have different insertion behaviors. The change in Zone II could be due to a charge transfer effect like in GIC occurring in the PPP-700 electrode, which would modify the localized electron density and electrical conductivity which is reflected to the final diminishing of the peaks. It is noteworthy also that even in the present very disordered structure of PPP-700, the same behavior as charge transfer in GIC can take place to store Li^+ ions between the defective carbon layers, and this result is phenomenologically consistent with the formation of Li_2 molecules [20]. On the other hand, Li storage in Zone I might be different from that occurred in Zone II. Though, it is still difficult to clarify the Li storage mechanism, it could be suggested that Li in Zone I may be firstly stored at preferred sites, and charge transfer affecting the peak wave number does not occur. Inaba et al. [34] reported the in situ Raman study on MCMB, heat-treated at around 1000°C, showed no change at the 1580 cm^{-1} Raman peak. These different results indicate that charge and discharge mechanism taking place especially in such a low temperature carbons with super high Li storage capacity should be different in each case, and is dependant upon the delicate structure of each of the carbons. It is difficult to explain systematically by the common scheme by the models which have been proposed [20–22].

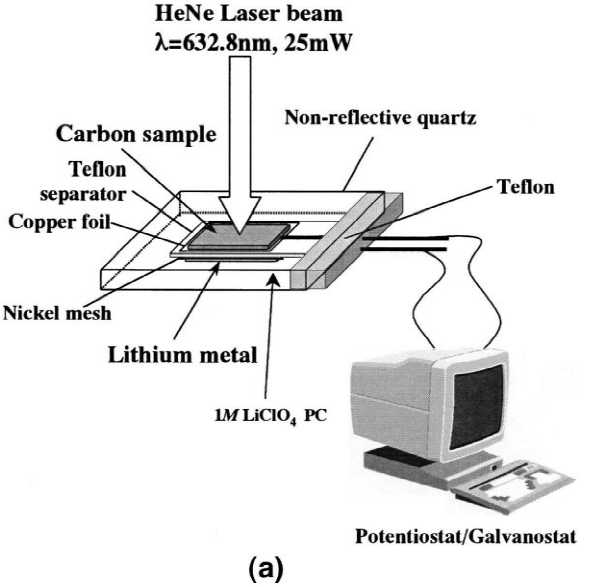

Fig. 10. (a) Schematic representation of the in situ Raman experiment, (b) in situ Raman spectra of PPP-700 heat treated at as low as 700°C, measured at various cell voltages for discharging from 2.8 to 0.04 V, and for charging from 0.04 to 2.74 V.

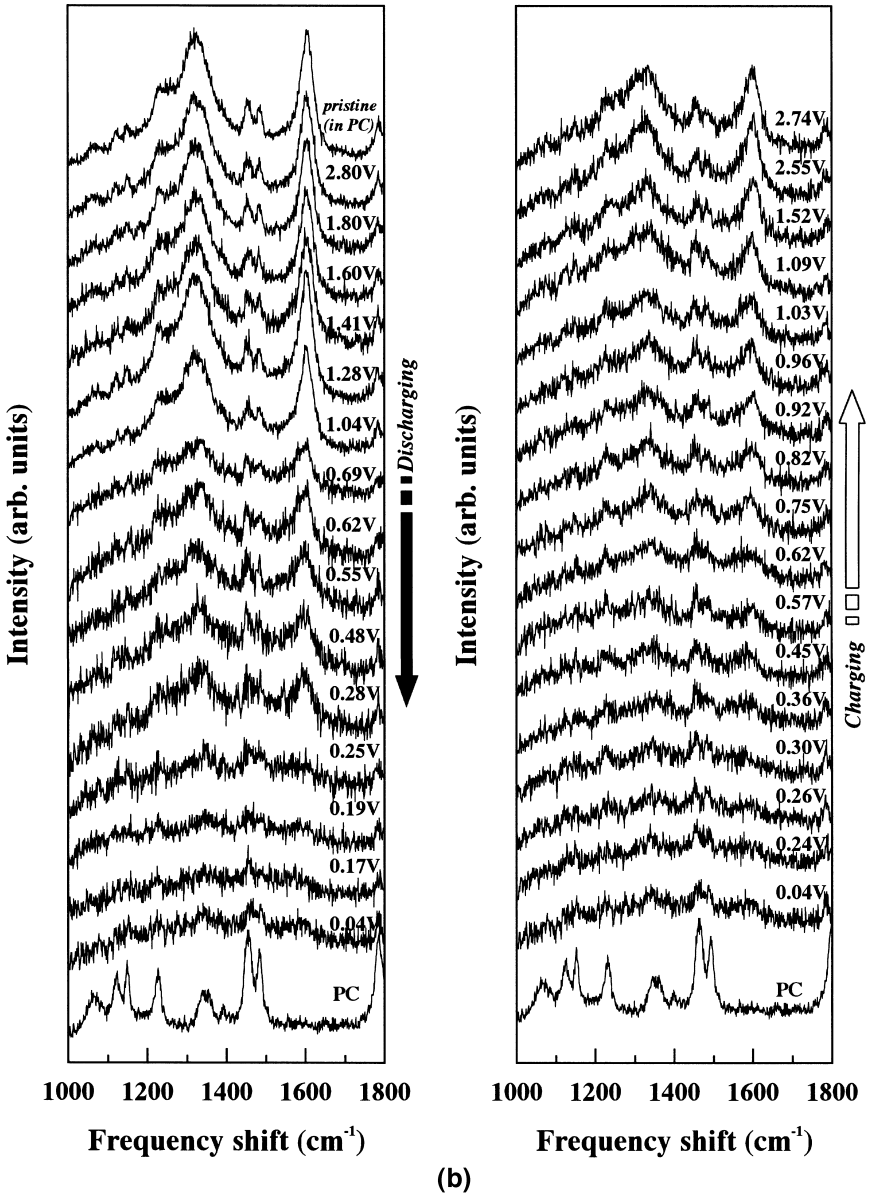

Fig. 10. (*continued*)

5. Effect of morphologies, carbon fibers for Li ion battery

Carbon fibers used for electrodes in lithium ion batteries are roughly classified into two types such as milled mesophase pitch-based carbon fibers and gas phase grown carbon fiber commonly called as vapor grown carbon fibers (VGCFs) [35]. The former is contributing as one of the practical and promising anode material with high density of electrode, larger discharge capacity and better output current performances. The latter can serve as conductive filler in anode and cathode electrodes. On the other hand, Endo [16] and Tatsumi [37] reported the battery characteristics of VGCF with wooden annual ring structure, and showed the interesting potential application as anode. Fig. 12a and b [38] demonstrates the SEM pictures of the thin VGCF obtained by the floating catalysis process and the graphite anode mixed with the fibers. The conductivity and cyclic life has been improved and this is very promising as one of the important technology of the battery.

The Li charge capacity and cyclic efficiency depends strongly on the cross sectional structure of the fibers, such as onion, radial and random structures [36,37]. In par-

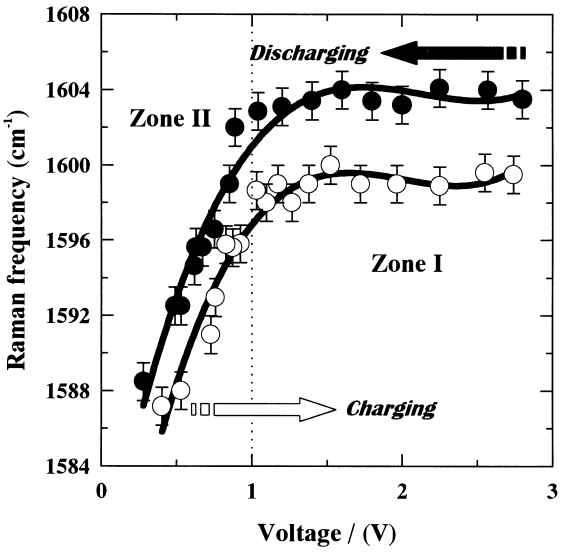

Fig. 11. The voltage dependences for the high frequency Raman modes of the PPP-700 electrode obtained by fits to Lorentzian line shape.

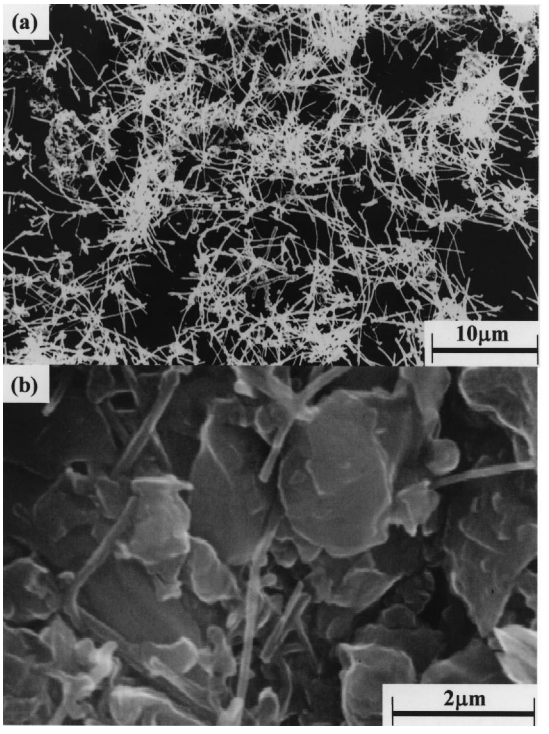

Fig. 12. (a) SEM photographs of the thin VGCF obtained by the floating catalysis process [35,38] and (b) the graphite anode mixed with the fibers in a commercial cell.

ticular, mesophase pitch-based carbon fibers (MPCFs) exhibit a high degree of anisotropy with regard to mechanical, electrical, magnetic, thermal as well as chemical properties [19,39]. These anisotropies are directly related to the layered structure with strong interlayer interactions and very weak van der Waals interplanar interactions between adjacent graphene sheets aligned parallel to the fiber axis [40]. The novel chemical and physical properties of the mesophase pitch-based carbon fibers have also been

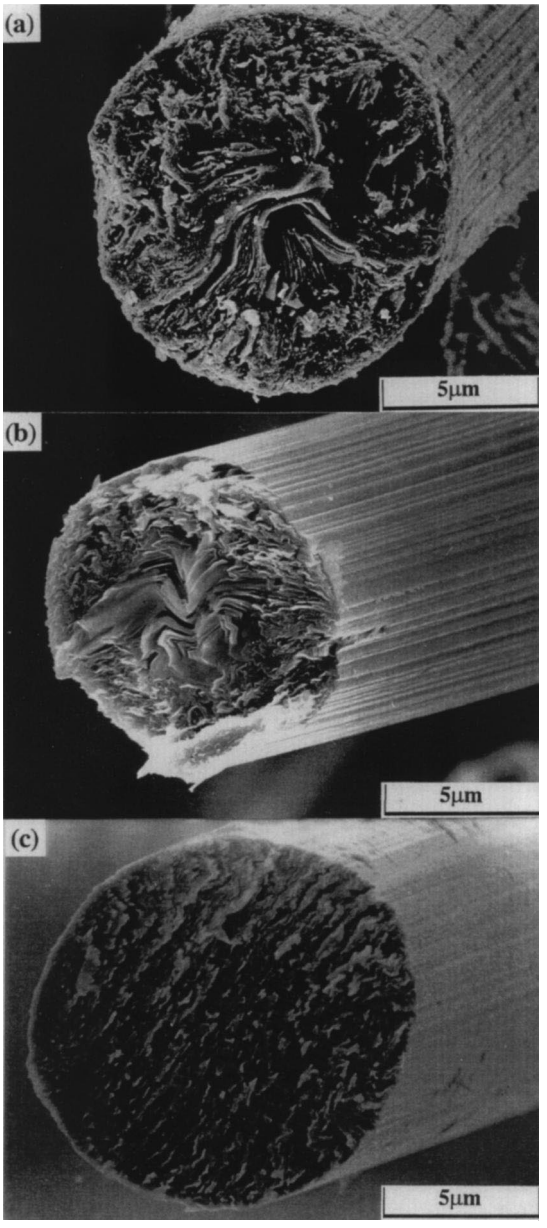

Fig. 13. FE–SEM photographs of milled MPCFs with HTT (a) 1000°C, (b) 3000°C, and (c) high modulus mesophase pitch-based graphite fiber (P-100).

utilized as a functional material in the new applications areas, especially for anode materials of Li ion batteries [36,41–46].

Fig. 13 shows typical FE–SEM images of milled MPCFs heat-treated at temperatures of 1000 and 3000°C, and these images are compared with those of conventional high modulus pitch-based carbon fiber (P-100) [40]. It has been known that each of the milled fibers of the present samples have very similar cross-sectional morphologies, in which the edge structure is only exposed at the cut end portion of the fibers. This controlled edge structure could account for the homogeneous and better electrochemical properties of the fibers in terms of charge capacities and cyclic efficiencies. As seen in Fig. 13, both fibers with different HTT also show a similar cross sectional texture, with a weakly developed radial structure (Fig. 13a and b). A morphological change was not observed after heat treatment. They show a plate-like texture with parallel alignment of the layers in the central part of the fiber, and at the peripheral region of the fiber the layers are more irregularly arranged. The present structure is very different from the conventional high modulus pitch-based carbon fibers as indicated in Fig. 13c, showing the parallel layer structure over the whole cross section of the fiber. It is also noteworthy that the cross sectional core region has a well-aligned layer structure, as demonstrated by the high magnification micrograph shown in Fig. 14a, while at the periphery (Fig. 14b), we can see a more wavy and less ordered layered structure, where the layers are arranged like bamboo shoots along the surface of the fiber. The cross sectional morphology of the present fibers is schematically demonstrated in Fig. 14c. These structural features with different morphologies in the cross section of the MPCFs might contribute to their superior properties as an anode material for a Li^+ inserted host material in Li ion batteries [44], while a homogeneous cross sectional morphology might be important for high performance in mechanical properties as in P100.

6. The factors restricting the capacity and effect of heteroatom-doped carbons

As the structural factors affecting the anode characteristics of graphite, especially the capacity less than the theoretical value of 372 mAh/g, the effects of the a–b axis crystallite size [45], stacking fidelity [21,46] and defect of the basal planes [44] have been proposed. Tatumi et al. [46] divided the discharge curve of graphitized MCMB at the threshold potential of 0.25 V, and evaluated the corresponding charge capacity as functions of graphitization degree and turbostratic components as shown in Fig. 15. It was shown that the capacity below 0.25 V was well related to the amount of the graphite structure component, P_1, and 0.25~1.3 V capacity depending upon the turbostratic one $(1-P_1)$. It has been difficult to eliminate perfectly the turbostratic and defect structure even in graphitizing carbons by heat treatment as high as 3000°C. In order to improve the capacity of these graphite systems, it could be interesting to dope the hetero atoms such as B, P and N in graphite materials [31].

Recently, heteroatom-doped carbon, such as BC_x, BC_xN and C_xN have been suggested for potential applications as anode materials in Li ion batteries, because these com-

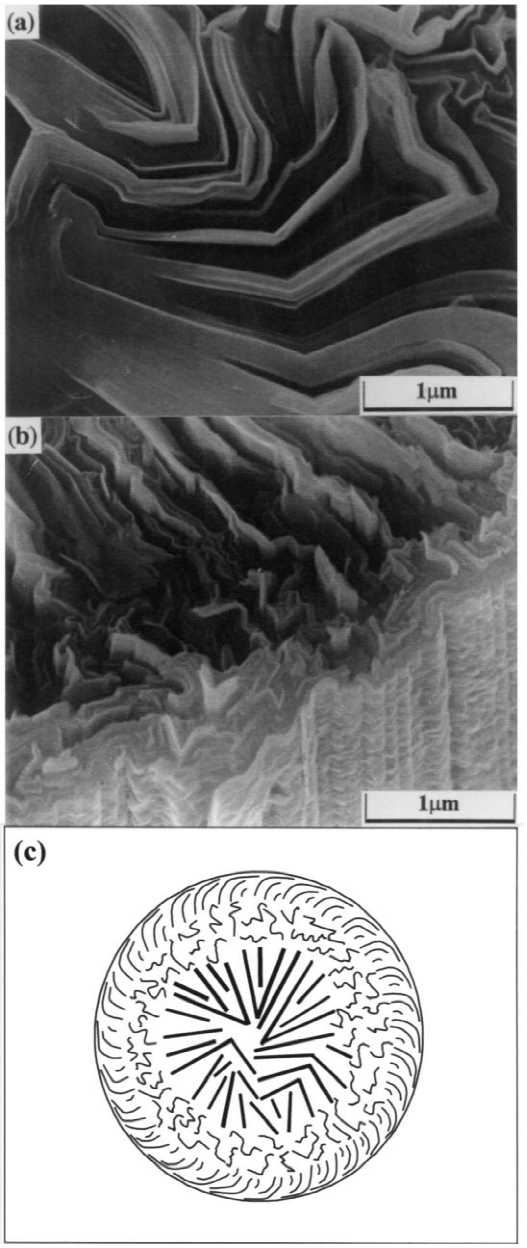

Fig. 14. SEM photographs of the (a) center and (b) periphery of an milled MPCF heat-treated at 3000°C and (c) a schematic layer model of the fibers.

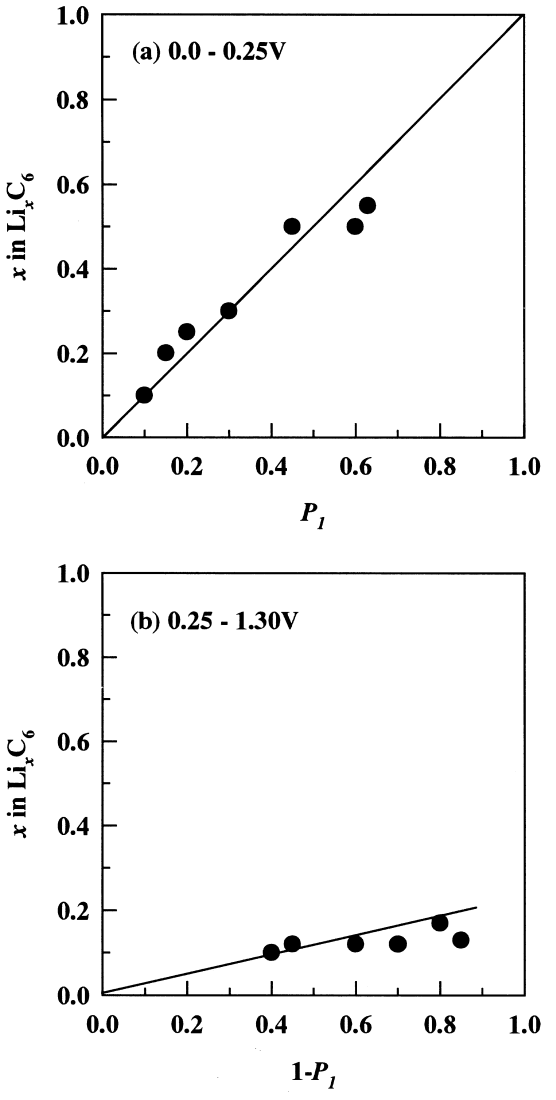

Fig. 15. The relationship linking the charge capacity of MCMBs during the first cycle and the volume ratio of the structures: (a) the charge capacity in the potential range of 0–0.25 V vs. P_1 plots; (b) the charge capacity in the potential range of 0.25–1.3 V vs. $(1-P_1)$ plots, referred from Tatsumi et al. [46].

pounds consist of layered structure [37,47,48]. In particular, boron-doped carbon materials have been experimentally and theoretically investigated from different points of view, not only from fundamental scientific aspects, such as electronic properties, but also towards potential applications, such as the high temperature oxidation protector for carbon/carbon (C/C) composite and an anode material for Li ion batteries. Because boron-doping is inducing the creation of electron acceptor level [37,47–50], the enhanced capacity has been expected. Many researchers [37,47–50] have reported and suggested preparative methods for boron-doped carbons by co-deposition of CVD pyrolysis of organic molecules containing boron atoms and the substitutional boron doping mechanism into carbon structures.

Fig. 16 illustrates the typical voltage profiles of the second discharge and charging for pristine graphitized and boron-doped electrodes. These samples were prepared from a mixture of pristine material and boron carbide (B_4C) by heat treatment at 2800°C in Ar atmosphere. The wide plateaus below 0.2 V correspond to the reversible intercalation of Li in graphitized and boron-doped samples. These electrochemical behaviors of the graphitized samples are almost the same as that of other highly graphitized electrodes [46,51]. It should be noted that the 2nd discharge-charge capacity of boron-doped graphite I (petroleum coke) and graphite II (carbon spheres) slightly decreased relative to those of the pristine samples. However, in the case of boron-doped MPCFs, the 2nd charge capacity is larger than that of undoped pristine MPCFs. The reduced charge capacity of the boron-doped samples may be related to boron atoms occupying the lithium

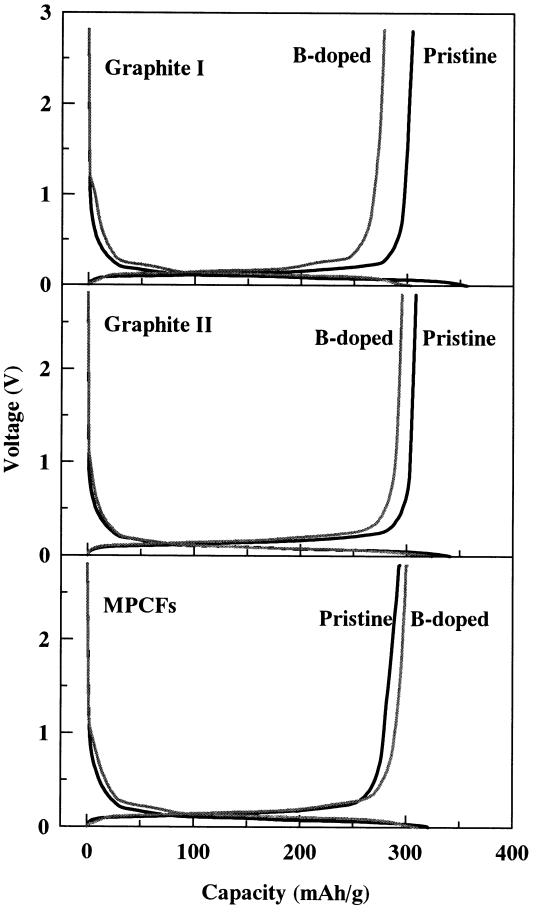

Fig. 16. Change in potential during the second discharging and charging cycle of the graphitized and boron-doped samples for various types of graphite hosts.

insertion active site, such as an edge-type site in the carbon layers and thus the presence of the boron will inhibit the lithium insertion process. Also, the discharge capacities of graphite I and graphite II are larger than that of MPCFs, because lithium insertion is easily accomplished in the wholly exposed edge surface of these carbons, relative to MPCFs. It is worthwhile to note that the voltage profiles of boron-doped samples are higher than those of the undoped samples at about 40 mV [36], and this could be useful for practical cell applications. On the discharging cycle for the boron-doped samples, shoulder plateau are characteristically observed at about 1.3 V, which may be caused by inducing an electron acceptor level so that lithium insertion yields a higher voltage compared to undoped samples [36,47]. The irreversible capacity is calculated as the average ratio of the capacities for the discharge and charge process. It is interesting that the irreversible capacity loss for boron-doped samples is lower than that of the corresponding undoped samples. These results may be related to the redistribution of the Fermi level of the boron-doped samples, which is lowered by boron-doping by introducing an electron acceptor in the lattice [36,47].

Fig. 17 shows the carbon 1s peak at high resolution XPS spectra. It is interesting that the C_{1s} peak of the boron-doped samples is located at slightly lower binding energy compared with the undoped samples. The lowering of the binding energy of the C_{1s} peak for the boron-doped samples might be due to the lowering of the Fermi level, because of the redistributed π-electrons in the graphite layer planes [52,53]. This result may be related to lowering the density of π electrons in the graphite layers, because of the chemical bond formation of carbon atoms with the electron deficient boron atom. Therefore, the C_{1s} peak of boron-doped samples moves to lowering the binding energies.

Figs. 18 and 19 illustrate the boron and nitrogen 1s peak in the XPS spectrum. As expected, the B_{1s} peak appears in the boron-doped samples, but their forms and positions are different, depending on the samples. In particular, the B_{1s} peak of the boron-doped graphite I was split into three peaks at 185.6, 187.7, and 189.8 eV, which were assigned to boron in boron carbide, in a boron cluster or boron bound to incorporated nitrogen atoms, respectively. And also, in Fig. 19 the N_{1s} peak is observed only in boron-doped Graphite I. From these results, the appearance of the B_{1s} near ~190 eV and N_{1s} near ~398 eV peaks of boron-doped Graphite I is corresponding to the substitutionally incorporated boron atoms into the graphite lattice which are preferentially bonding with nitrogen atoms existing in the heat treatment atmosphere. It is also possible that the residual nitrogen atoms in raw materials react with the substitutionally incorporated boron atoms into the graphite lattice during the carbonization step and then formed the boron nitride and/or BC_xN compounds during the graphitization step. Konno et al. [54] demonstrated the B–N bonding in boron doped graphites by XPS and suggested

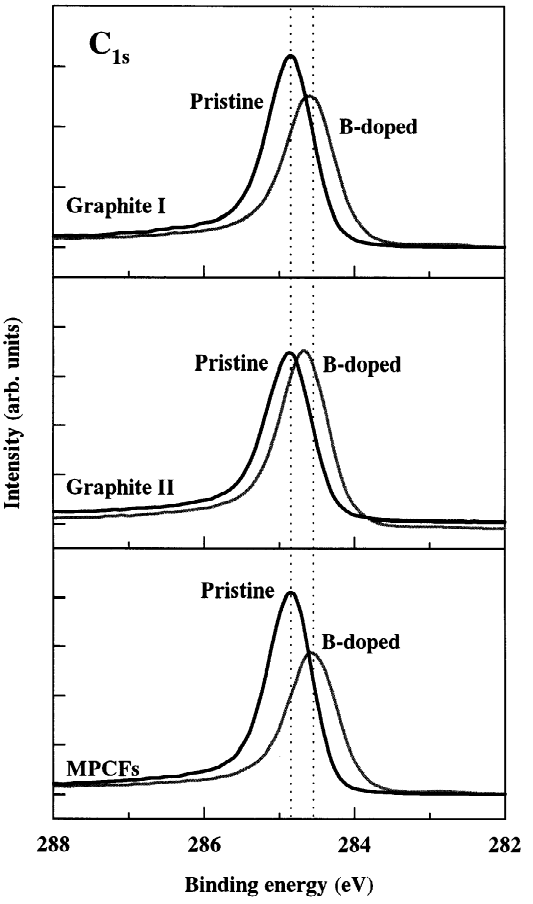

Fig. 17. XPS C_{1s} spectra of graphitized and boron-doped samples for various types of graphite hosts.

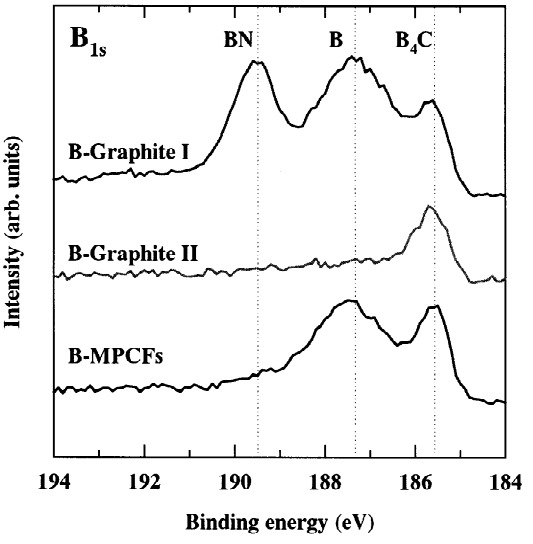

Fig. 18. XPS B_{1s} spectra of boron-doped samples.

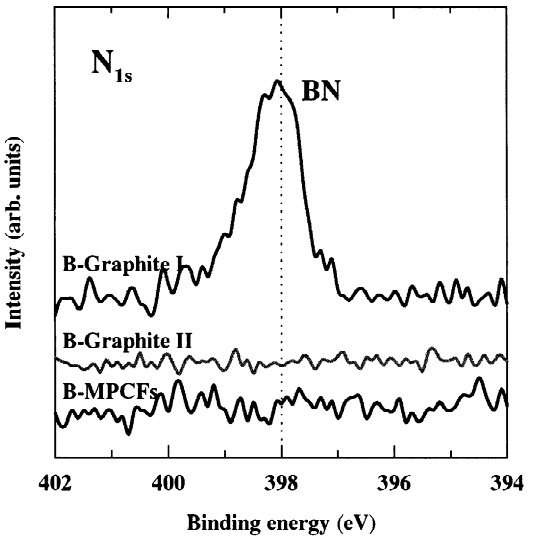

Fig. 19. XPS N_{1s} spectra of boron-doped samples.

the possible nitrogen source as air occluded in raw materials that are packed into a graphite crucible. These phenomena should be taken into consideration seriously for industrial process using an Acheson type furnace.

As mentioned above, the degradation of the lithium insertion capacity observed in some kinds of boron-doped graphite might be highly related to the presence of borons in forms of boron nitride and boron carbide. Also the unexpected opposite effects of boron doping could be related to the heterogeneous growth of the crystallites

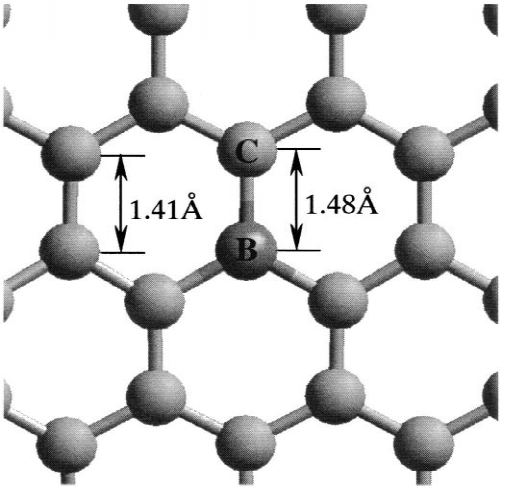

Fig. 20. Schematic representation of a graphene plane of the boron doped MPCFs. The difference in bond length between a B–C and C–C bond is indicated [49].

dimension, L_a, due to the borons acting as a graphitization catalyst. On the other hand, boron-doping in MPCFs can induce the homogeneous crystallite ordering, approaching to the ideal graphite structure, as indicated by the XRD, XPS, and Raman results [55]. Fig. 20 shows a proposed schematic model of a graphite plane in which the substitutional boron atoms show different bond lengths between the B–C and C–C bonds. Data from a molecular simulation are shown in the figure [49]. In order to better employ the effects of boron doping, depending on the carbon materials obtained from a different precursor with a wide variety of shapes and microstructure, the doping conditions including the atmosphere and heating rate should be carefully selected. This could provide one of the new types of material design of carbon or graphite electrodes.

7. Polymer battery

The name of ''polymer battery''is defined like the battery which has a polymer electrode and/or electrolyte. Very recently, a Li ion battery with gel type polymer electrolyte has been commercialized which is only 3.6 mm thick, weighs 15 g and has a capacity of 500 mAh, as shown in the Table 1 [56]. The gel electrolyte consists of poly(ethylene oxide) (PEO), poly(acrylonitrile) (PAN), and poly(vinylidene fluoride) (PVdF) as the host polymer, EC/PC as the plasticizer and $LiPF_6$ as the electrolyte salt. This film or card shaped battery has energy density in volume and weight of 250 Wh/l and 120 Wh/kg, respectively, which is almost equivalent with those of the conventional cylindrical cell. No inclusion of liquid electrolyte increases the safety and can contribute to reducing the cell thickness and weight. The same types of graphitic anode materials as in the conventional cylindrical cell have been used. Formation of the anode film with suitable density and porosity to permit a high degree of penetration of gel in the electrodes and enough conductivity should be achieved. These polymer batteries could reduce the thickness of cellular phones and portable PCs (see Table 1, Fig. 21a and b, and Ref. [56]).

Table 1
Specifications of a commercialized Li polymer battery [56]

Production	Lithium polymer battery
Model No.	SSP356236
Shape	Prismatic
Size	$35(W)\times62(L)\times3.6(T)$ mm
Voltage	3.7 V
Average electric capacity	500 mAh (charged at 4.2 V)
Weight	Approximately 15.0 g
charge–discharge cycles	500 cycles or more
Working temperature range	$-10\sim+60$°C

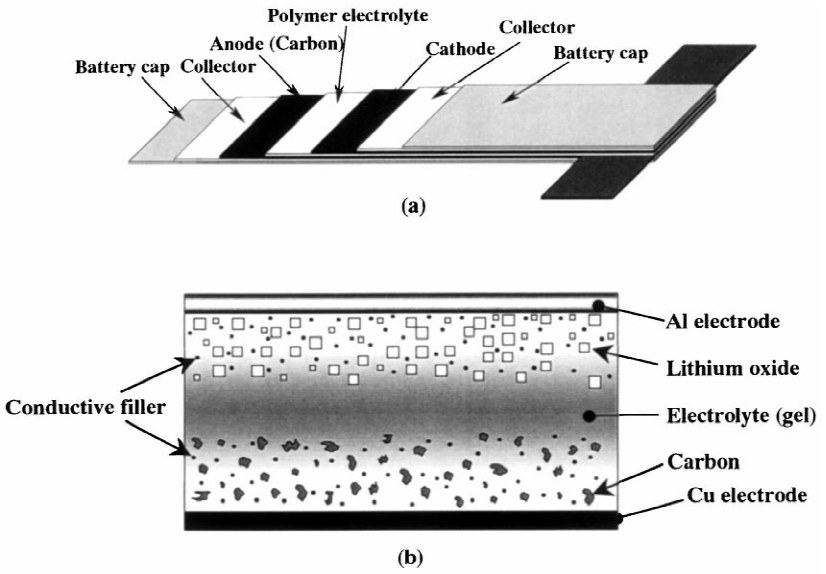

Fig. 21. The configuration of polymer Li ion battery (a) and basic composition of the practical electrode (b) [56].

8. Conclusions and prospects

It is not an overstatement that the success of the Li ion batteries has been contributed to by the advancements in GIC and carbon sciences made before to the early 1990s. They had been able to provide newly designed anode materials for the batteries. Enhancement of the battery performances and cost reduction have been also achieved in past 7 years, and now further improvements in performances of the battery is necessary for future development. On the low temperature carbons with high capacities, elucidation of the storage mechanism of Li and improvement on the irreversible capacity are important keys factors. And further research on the carbonization and graphitization conditions of new starting materials as well as some additives such as B, N and P involving mechanical treatment will be required. Fig. 22 shows the comparison of the energy density in various kinds of batteries, which indicates the predominance of Li ion batteries. A remarkable improvement in Li ion batteries will progress in the future so that the Li metal itself will be approached, but carbon and graphite being such low crystalline carbons can expect higher capacities. The expectation for carbon and graphite as anode materials should be strengthen more and more from now on. Taking all these factors in to account, carbon as well as the intercalation sciences will greatly be able to contribute to the further development of Li ion batteries as the second and third generation of the battery will be soon coming. High performance Li ion battery with advanced carbons will be required more in the coming 21st century of multimedia, wearable computers and environmental awareness.

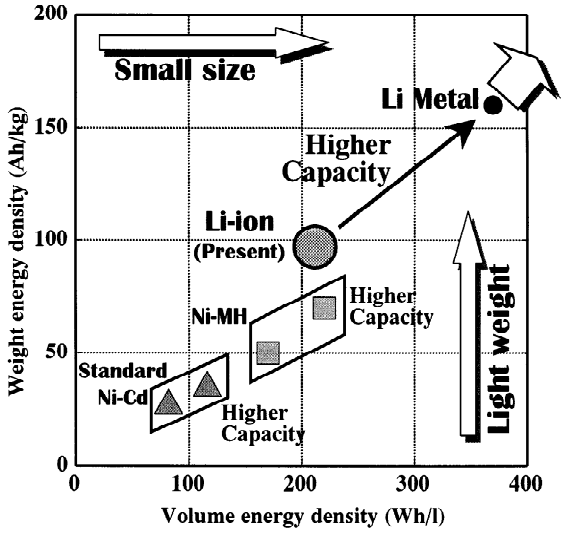

Fig. 22. The recent capacity improvement and future possibility of Li ion and other secondary batteries.

Acknowledgements

This research was partially supported by the Ministry of Education, Science Sports and Culture, Grant-Aid for Scientific Research on Priority Area (Carbon Alloys), No. 09243105. The author (M.E) wishes to thank Prof. M. S. Dresselhaus of MIT for helpful suggestion and discussion.

References

[1] Gabano JP. In: Lithium batteries, New York: Academic Press, 1983.
[2] Armand MB. In: Van Gool W, editor, Fast ion transport in solids, Elsevier, 1973, p. 665.
[3] Murphy DW, Carides JN. J Electrochem Soc 1979;126:349.
[4] Lazzari M, Scrosati B. J Electrochem Soc 1980;127:773.
[5] Auborn JJ, Barberio YL. J Electrochem Soc 1987;134:638.
[6] Herold A. Bull Soc Chim France 1955;187:999.
[7] Juza R, Wehle V. Nature 1965;52:560.
[8] Guerard D, Herold A, Acad CR. Sci Ser 1972;C275:571.
[9] Dahn JR, Fong R, Spoon JJ. Phy Rev 1990;B42:6424–32.
[10] Dresselhaus MS, Dresselhaus G. Adv in Phys 1981;30:139.
[11] Semenenko KN, Avdeev VV, Mordkovich VZ, Doklady AN. SSSR 1983;271:1402, In Russian.
[12] Avdeev VV, Nalimova VA, Semenenko KN. High Pressure Research 1990;6:11.
[13] Sony's catalog, Lithium ion rechargeable battery, ACG-4012-N-9707-P3-002, 1997.
[14] Endo M, Karaki T, Fujino T. New ceramics 1998;4:46–52, (In Japanese).
[15] Yata S, Kinoshita H, Komori M, Ando N, Anekawa A, Hashimoto T. In: Extended abstract of 60th annual meeting of the electrochemical society of Japan, Tokyo, 2G09, 1993.
[16] Endo M, Nishimura Y, Takahashi T, Takeuchi K, Dreselhaus MS. J Phys Chem Solids 1996;57:725–8.
[17] Oberlin A. In: Thrower PA, editor, Chemistry and physics of carbon, Vol. 22, New York: Marcel Dekker, Inc, 1989, p. 1.
[18] Imanishi N, Kashiwagi H, Ichikawa T, Takeda Y, Yamamoto O, Inagaki M. J Electrochem Soc 1993;140:315–20.
[19] Dresselhasu MS, Dresselhaus G, Sugihara K, Spain IL, Goldberg HA. In: Cardona Manuel, editor, Graphite fibers and filaments, New York: Springer-Verlag, 1988.
[20] Sato K, Noguchi M, Demachi A, Oki N, Endo M. Science 1994;264:556–8.
[21] Dahn JR, Zheng T, Liu Y, Xue JS. Science 1995;270:590–3.
[22] Mabuchi A, Tokumitsu K, Fujimoto H, Kasuh T. J Electrochem Soc 1995;142:1041–6.
[23] Dahn JR. Phys Rev 1991;B44:9170–7.
[24] Flandrois S, Simon B. Carbon 1999;37:165–80.
[25] Funabiki A, Inaba M, Ogumi Z, Yuasa S, Otsuji J, Tasaka A. J Electrochem Soc 1998;145:172–8.
[26] Nagaura T, Tozawa K. Prog Batt Solar Cells 1990;9:209.
[27] CMC, Development of Li-ion Rechargeable Battery Materials, Tokyo, CMC, 1998, p. 149 (in Japanese).
[28] Data from Battery Association of Japan, 1997, 1998.
[29] Fong F, Sacken Kvon, Dahn JR. J Electrochem Soc 1990;137:2009–13.
[30] Buiel E, George AE, Dahn JR. J Electrochem Soc 1998;145:2252–7.
[31] Dahn JR, Sleigh AK, Shi H, Way BM, Weycanz WJ, Reimers JN, Zhong Q, von Sacken U. In: Pistoia G, editor, Lithium batteries, new materials and perspectives, Amsterdam: Elsevier, 1993, p. 1.
[32] Yoshino A. Tanso 1999;186:45–9, In Japanese.
[33] Endo M, Kim C, Karaki T, Fujino T, Matthews MJ, Brown SDM, Dresselhaus MS. Synthetic Metals 1998;98:17–24.
[34] Inaba M, Yoshida H, Ogumi Z. J Electrochem Soc 1996;143:2572–8.
[35] Endo M. Chemtech 1988;18:568–76.
[36] Nishimura Y, Yakahashi T, Tamaki T, Endo M, Dresselhaus MS. Tanso 1996;172:89–94, In Japanese.
[37] Tatsumi K, Zaghib K, Sawada Y, Abe H, Ohsaki T. J Electrochem Soc 1995;142:1090–6.
[38] Showa denko's catalog, Fine Carbon, V.G.C.F., 1997.
[39] Matthews MJ, Dresselhaus MS, Dresselhaus G, Endo M, Nishimura Y, Hiraoka T, Tamaki T. Appl Phys Lett 1996;69:430.
[40] Endo M, Kim C, Karaki T, Kasai T, Matthaus MJ, Brown SDM, Dresselhaus MS, Tamaki T, Nishimura Y. Carbon 1998;36:1633–41.
[41] Tamaki N, Satoh A, Hara M, Ohsaki T. J Electrochem Soc 1995;142:2564–71.
[42] Satoh A, Tamaki N, Ohsaki T. Solid State Ionics 1995;80:291.
[43] Ohsaki T, Kanda M, Aoki Y, Shiroki H, Suzuki S. J Power Sources 1997;68:102.
[44] Endo M, Nakayama J, Sasabe Y, Takahashi T, Inagaki M. Tanso 1994;165:282–7, In Japanese.
[45] Fujimoto H, Mabuchi A, Tokumitsu K, Kasuh T, Akuzawa N. Carbon 1994;32:193–8.
[46] Tasumi K, Iwashita N, Sakaebe H, Shioyama H, Higuchi S, Mabuchi A, Fujimoto H. J Electrochem Soc 1995;142:716–20.
[47] Way BM, Dahn JR. J Electrochem Soc 1994;141:907–12.
[48] Nakajima T, Koh K, Takashima M. Electrochimica Acta 1998;43:883–91.
[49] Endo M, Kim C, Karaki T, Tamaki T, Nishimura Y, Matthews MJ, Brown SDM, Dresselhaus MS. Phy Rev 1998;B58:8991–6.
[50] Hagio T, Nakamizo M, Kobayashi K. Carbon 1989;27:259–63.
[51] Koh K, Nakajima T. Carbon 1998;36:913–20.
[52] Henning G. J Chem Phy 1965;42:1167–72.
[53] Jones LE, Thrower PA. Carbon 1991;29:251–69.
[54] Konno H, Nakahashi T, Inagaki M, Sogabe T. Carbon 1999;37:471–5.
[55] Endo M, Kim C, Fujino T, Dresselhaus MS, to be submitted.
[56] National/Panasonic catalog, 1999 (courtesy of Matsushita Battery Industrial Co., Ltd.).